ISME

Check for updates

ARTICLE
Potential for mercury methylation by Asgard archaea in mangrove sediments

Cui-Jing Zhang [1,2,6], Yu-Rong Liu [3,6], Guihong Cha[4], Yang Liu [1,2], Xin-Quan Zhou[3], Zhongyi Lu[1,2], Jie Pan [1,2], Mingwei Cai [1,2,5] and Meng Li [1,2✉]

Methylmercury (MeHg) is a potent neurotoxin that bioaccumulates along food chains. The conversion of MeHg from mercury (Hg) is mediated by a variety of anaerobic microorganisms carrying *hgcAB* genes. Mangrove sediments are potential hotspots of microbial Hg methylation; however, the microorganisms responsible for Hg methylation are poorly understood. Here, we conducted metagenomic and metatranscriptomic analyses to investigate the diversity and distribution of putative microbial Hg-methylators in mangrove ecosystems. The highest *hgcA* abundance and expression occurred in surface sediments in Shenzhen, where the highest MeHg concentration was also observed. We reconstructed 157 metagenome-assembled genomes (MAGs) carrying *hgcA* and identified several putative novel Hg-methylators, including one Asgard archaea (Lokiarchaeota). Further analysis of MAGs revealed that Deltaproteobacteria, Euryarchaeota, Bacteroidetes, Chloroflexi, and Lokiarchaeota were the most abundant and active Hg-methylating groups, implying their crucial role in MeHg production. By screening publicly available MAGs, 104 additional Asgard MAGs carrying *hgcA* genes were identified from a wide range of coast, marine, permafrost, and lake sediments. Protein homology modelling predicts that Lokiarchaeota HgcAB proteins contained the highly conserved amino acid sequences and folding structures required for Hg methylation. Phylogenetic tree revealed that *hgcA* genes from Asgard clustered with fused *hgcAB* genes, indicating a transitional stage of Asgard *hgcA* genes. Our findings thus suggest that Asgard archaea are potential novel Hg-methylating microorganisms and play an important role in *hgcA* evolution.

INTRODUCTION

Due to natural processes and anthropogenic effects, mercury (Hg) is widespread in terrestrial and aquatic ecosystems such as sediments, rice paddy soils, and the water column [1]. Inorganic Hg in the environment can be converted to potent neurotoxic methylmercury (MeHg) by a variety of anaerobic microorganisms [2, 3]. The synthesized MeHg can subsequently bioaccumulate and biomagnify in food chains, posing a risk to wildlife and to human health [4]. Therefore, it is critical to investigate MeHg production and Hg-methylating microorganisms in aquatic environments.

The *hgcAB* gene cluster provides a molecular marker for identifying Hg-methylating microorganisms [5]. The *hgcA* gene encodes a homolog of corrinoid iron-sulfur proteins, and the *hgcB* gene is generally present next to *hgcA* by encoding an iron-sulfur cluster protein in various microorganisms including bacteria and archaea [6]. Previous structure model of the HgcB suggested that conserved cysteines in HgcB are involved in shuttling Hg[II], methymercury, or both [7]. The gene pair *hgcAB* presumably functions in methyltransferase and corrinoid reduction, endowing microorganisms with the ability to produce MeHg [5]. All experimentally confirmed Hg-methylators contain *hgcA* homologues, which predominantly affiliate to sulfate-reducing bacteria

and iron-reducing bacteria belonging to the class δ-Proteobacteria within the phylum Proteobacteria, fermentative bacteria within the phylum Firmicutes (Clostridia), and methanogenic archaea within the phylum Euryarchaeota [8, 9]. More diverse *hgcA* carriers, including Chloroflexi, Spirochaetes [10], Nitrospina [11], Planctomycetes, Verrucomicrobia [12], Acidobacteria, Actinobacteria, Aminicenantes, Elusimicrobia, and Nitrospirae [6, 13–15] have been discovered in other microbial phyla using culture-independent approaches. It is believed that microorganisms carrying *hgcAB* gene sequences are phylogenetically diverse and prevalent in a wide range of habitats [16, 17].

Asgard is a recently discovered archaeal superphylum that contains more than 16 distinct phyla, such as Loki-, Thor-, Odin-, Heimdall-, Hel-, Gerd-, Sif-, Baldr-, Hermod-, Borr-, Hod-, Kari-, Wukong-, Sigyn-, Freyr- and Njordarchaeota [18–25]. They are widely distributed in anoxic environments such as sediments, cold seeps, hot springs, and soils [26–28]. Previous surveys have revealed high concentrations of heavy metals (e.g., Cu, Pb, Hg, As) in certain anoxic wetlands, lake, marine, and paddy sediments [29–31]. These findings imply that Asgard archaea can adapt to sediment conditions with high concentrations of heavy metals, suggesting that they are involved in heavy metal

[1]Archaeal Biology Center, Institute for Advanced Study, Shenzhen University, 518060 Shenzhen, China. [2]Shenzhen Key Laboratory of Marine Microbiome Engineering, Institute for Advanced Study, Shenzhen University, 518060 Shenzhen, China. [3]State Key Laboratory of Agricultural Microbiology, Huazhong Agricultural University, 430070 Wuhan, China. [4]Key Laboratory of Development and Application of Rural Renewable Energy, Biogas Institute of Ministry of Agriculture and Rural Affairs, Chengdu, China. [5]Present address: Chemical Biology Institute, Shenzhen Bay Laboratory, Shenzhen, China. [6]These authors contributed equally: Cui-Jing Zhang, Yu-Rong Liu. ✉email: limeng848@szu.edu.cn
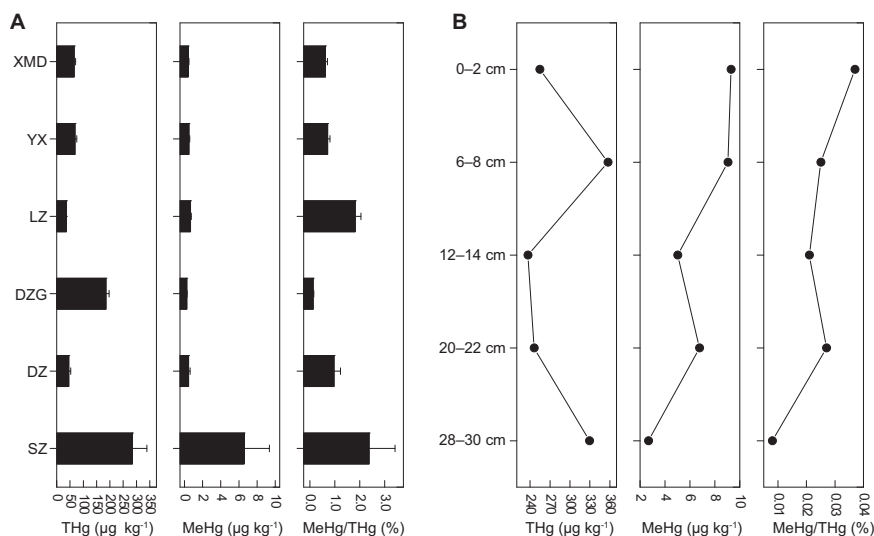
Fig. 1 Mercury profiles in mangrove sediments. A Concentrations of total Hg (THg), MeHg and MeHg as a percentage of THg at different sites. **B** Concentrations of total Hg (THg), MeHg and MeHg as a percentage of THg at different depths in Shenzhen.

metabolism [32]. However, whether Asgard archaea are able to methylate Hg remains unknown.

Mangroves, as hotspots of microbial Hg methylation, are ideal niches in which to search for novel putative Hg-methylators [33]. Mangrove sediments receive Hg inputs of anthropogenic origin as a substantial source for methylation [34–36]. In addition, abiotic factors such as relatively warm temperatures and low oxygen and high carbon contents in mangrove sediments could accelerate MeHg production by facilitating the activity of microbial methylators [29, 37, 38]. In this study, we measured the concentrations of total mercury (THg) and MeHg and applied metagenomic and metatranscriptomic analyses to investigate Hg-methylating microorganisms in the sediments of mangrove ecosystems across southeastern China (Fig. S1). We provide evidence of the potential novel Hg-methylators and their key roles in *hgcA* evolution.

RESULTS AND DISCUSSION
Hg and MeHg biogeochemistry in mangroves
Total Hg (THg) and MeHg concentrations in mangrove sediments are listed in Fig. 1 and Table S1. The concentrations of THg ranged from 36 to 357 µg kg^{-1} dry sediment, and MeHg ranged from 0.25 to 9.3 µg kg^{-1} dry sediment. Similar MeHg concentrations have been reported in other sediments [29]. Of all the sampling sites, Shenzhen (SZ) had the highest concentrations of THg and MeHg, which might be due to intensive anthropogenic emissions, such as wastewater discharge, that increase the Hg accumulation in mangrove sediments in Shenzhen [33]. In addition, the ratio of MeHg to THg decreased from 3.65% in surface (0–2 cm) sediments to 0.81% in bottom (28–30 cm) sediments in Shenzhen mangroves, suggesting a stronger activity of Hg-methylating microorganisms in the top sediments.

Identification of putative mercury-methylating microorganisms in mangrove sediments
By hidden Markov model (HMM) search, we identified a final set of 1087 *hgcA* genes from 10 mangrove metagenomic assemblies (Table S2). Among these, 706 *hgcA* gene sequences had downstream *hgcB* genes, suggesting that these are likely functional Hg-methylation genes. HgcA sequences that binned to MAGs were assigned taxonomic classifications according to GTDB taxonomy of MAGs phylogenies. Those HgcA sequences that not binned to MAGs were searched against reference HgcA and HgcAB sequences database published recently [39] using BLASTp (Table S3). The 1087

identified *hgcA* sequences were clustered into 28 phyla (Table S2). According to the phylogeny, HgcA sequences from the same taxonomy were not clustered into one clade (Fig. S2), which might be due to horizontal gene transfer (HGT) [40, 41]. The *hgcA* gene abundances varied among different sites and were highest in Shenzhen (Fig. S3), suggesting that Hg-methylators were most abundant at this site. Moreover, the transcripts of *hgcA* genes were highest at 6–8 cm in Shenzhen, suggesting that Hg-methylators were more active in subsurface sediment layers. We further found that some environmental factors (pH, Cl$^-$, and SO$_4^{2-}$ concentrations) were significantly correlated to MeHg/THg ratio (Fig. S4). It is widely accepted that TOC and pH affect Hg bioavailability and methylators' activities [42–44]. Indeed, previous studies had suggested that lower pH could increase Hg mobility and provide more available Hg for microbial Hg methylation [45]. We also observed a significantly positive correlation between the RPKM (reads per kilobase of transcript per million mapped reads) values of *hgcA* genes and MeHg/THg ratio ($p < 0.01$). Further correlation analysis showed that the most abundant mercury methylators such as Deltaproteobacteria, Chloroflexi, Planctomycetes, Spirochaetes, Nitrospirae, Euryarchaeota were significantly correlated with MeHg/THg ratio (Fig. S5), suggesting all these microorganisms play important roles in mercury methylation. Overall, the most abundant *hgcA* genes were observed in subsurface sediments of Shenzhen, where they coincided with the MeHg peaks. Since large amounts of terrestrial and riverine Hg reach and accumulate in coastal environments, the top layers of the mangrove sediments supply substrates for Hg-methylators [36, 46].

A total of 1183 MAGs with completeness >50% and contamination <10% were recovered from 10 mangrove metagenomics datasets after dereplication. Among these, 157 MAGs belonging to 20 groups at phylum level (Acidobacteria, Armatimonadetes, Bacteroidetes, Bathyarchaeota, Chloroflexi, Edwardsbacteria, Eisenbacteria, Euryarchaeota, Fibrobacteres, Gemmatimonadetes, Krumholzibacteriota, KSB1, Lokiarchaeota, Nitrospirae, Planctomycetes, Proteobacteria, Spirochaetes, TA06, WOR-3, Zixibacteria) have *hgcA* genes (Fig. 2A). Genome size, completeness, and contamination of the 157 MAGs are summarized in Table S4. Among these, 139 MAGs had an *hgcB* sequence paired with *hgcA*. Well-known methylators Deltaproteobacteria and Euryarchaeota accounted for 81 and 7 MAGs, respectively, representing more than one-half of all identified putative methylators. Putative methylators belonging to the Acidobacteria, Bacteroidetes, Chloroflexi, Eisenbacteria, Fibrobacteres, KSB1, Nitrospirae, Planctomycetes, Spirochaetes, TA06, and
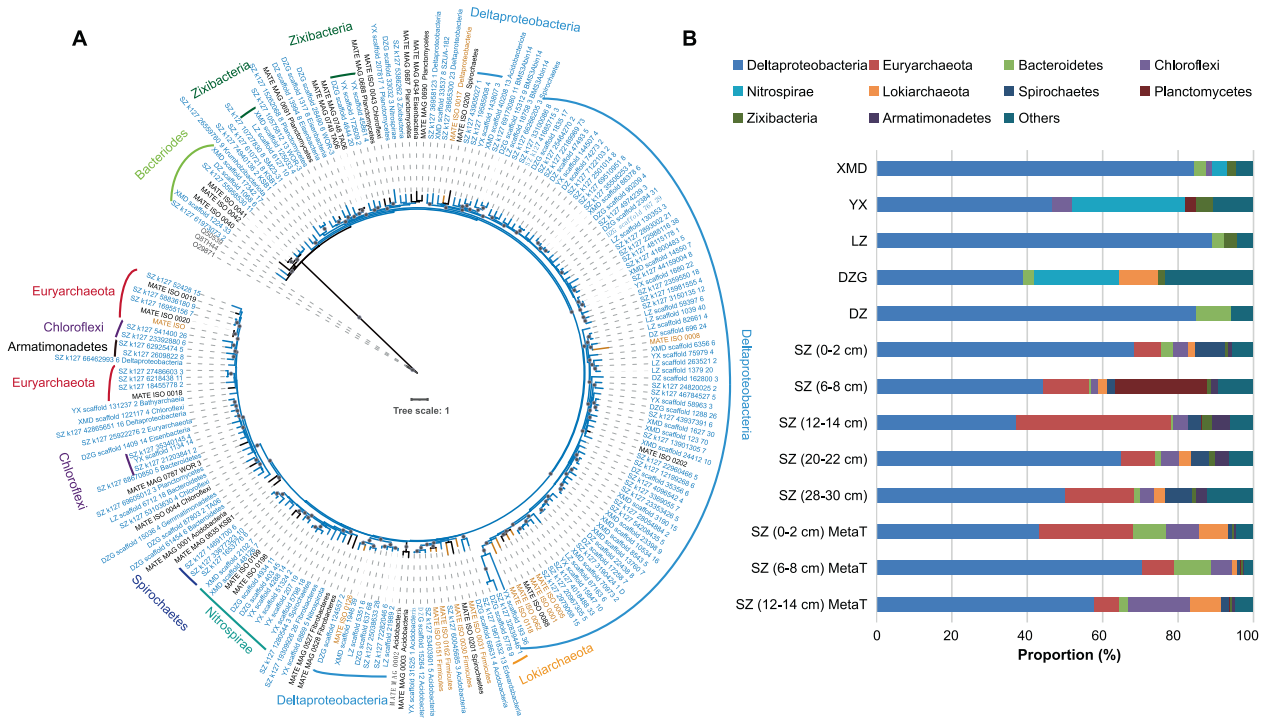
Fig. 2 Summary of 157 Metagenome-Assembled Genomes (MAGs) recovered with *hgcA* from mangrove sediments. A Maximum-likelihood phylogenetic tree of HgcA amino acid sequences (1000 bootstraps; values >90% are shown by gray dots at the nodes). The 157 HgcA sequences from corresponded MAGs (Table S4) obtained in this study are highlighted in blue. HgcA sequences retrieved from public databases are shown in black. Experimentally confirmed HgcA are shown in brown. HgcA paralogues from non-methylating microorganisms were used as outgroups and are shown in gray. **B** Relative abundances of *hgcA*-carrying MAGs affiliated to different taxonomic groups in different mangrove sediment samples. Different taxonomic groups are represented by different colors. MetaT represent metatranscriptomic.

WOR-3 have previously been identified from isolate genomes or reconstructed MAGs [6]. We also detected *hgcA* in phyla that, to our knowledge, have not previously been shown to carry the genes. These phyla include two bacterial phyla (Armatimonadetes and Gemmatimonadetes), two candidate archaeal phyla (Bathyarchaeota and Lokiarchaeota), and three candidate bacterial phyla (Edwardsbacteria, Krumholzibacteriota, and Zixibacteria). The most abundant putative Hg-methylator was Deltaproteobacteria, followed by Euryarchaeota, Bacteroidetes, Chloroflexi, Nitrospirae, and Lokiarchaeota (Fig. 2B). Deltaproteobacteria were abundant and active in all the samples, showing that they are predominant and widespread Hg-methylators across all mangrove sediments in Southeastern China. Previous studies have also shown that Deltaproteobacteria are the most abundant Hg-methylators in coastal sediments [10, 14]. In the present study, Desulfatiglandales, Desulfobacterales, Desulfobulbales, Desulfuromonadales, and Syntrophobacterales were the most frequent and abundant five orders in Deltaproteobacteria (Table S4). The relative abundances of Euryarchaeota *hgcA*-carriers were highest in the Shenzhen (SZ) site. Within Chloroflexi, *hgcA*-carriers were all in the Anaerolineae class, while experimental confirmation of Hg-methylation capacity in this phylum is still needed. Nitrospirae *hgcA*-carriers were more abundant in Yunxiao (YX), which is characterized by high nitrate concentration and nitrite oxidation rates [47]. The relative abundances of Lokiarchaeota *hgcA*-carriers account for 10 and 8% of the total *hgcA*-containing MAGs reads in Dongzhaigang and Shenzhen, respectively (Fig. 2). Our findings suggest a broad diversity of putative Hg-methylators.

The potential for Hg methylation by Asgard archaea
In this study, we identified *hgcA* gene sequence in Lokiarchaeota MAGs (DZG_bin1.240 and SZ_1_bins.287) (Table S4). To investigate the Hg methylation potentials of Asgard MAGs, we searched publicly available Asgard MAGs and obtained 104 Asgard MAGs that contain *hgcA* gene (Table S5). The 104 *hgcA*-carrying Asgard MAGs comprised 8 phyla: Borr-, Kari-, Hod-, Heimdall-, Loki-, Hel-, Hermod-, and Thorarchaeota, respectively. Asgard HgcA sequences contained the conserved NVWCAA motif (or is NVWCGA in one genome of Lokiarchaeota) in the cap helix (Fig. S6). Asgard HgcB sequences contained two tandem CX2CX2CX3C motifs (Fig. S6). To eliminate the possibility of contamination, all genes identified on the contigs containing *hgcA* genes in Asgard MAGs were blast against 201,003 Asgard amino acid sequences downloaded from NCBI as references (Table S6). All the identity of blast results were above 20% and 3318 of 3743 sequences were above 50%, suggesting these genes on the contigs likely belong to Asgard archaea.

Asgard archaea have never been implicated as putative methylators. The complete genome of the only one co-cultured representative of Lokiarchaeota archaea, *Candidatus* Prometheoarchaeum syntrophicum strain MK-D1 [48], showed that it contained *hgcAB* genes. However, it has not been experimentally tested for Hg-methylation capacity. Based on its HgcAB protein sequence and structure, we propose Lokiarchaeota as a potential mercury methylator. Homology models were constructed to predict the three-dimensional structure of Lokiarchaeota HgcA and HgcB amino acid sequences (Fig. 3A and B). Lokiarchaeota HgcA protein structure consisted of a corrinoid binding domain at the N-terminus and five transmembrane spanning helices at the C-terminus. The ligand cobalamin facilitates the transfer of methyl groups to inorganic Hg [49]. This structure is similar to the previously reported HgcA from the experimentally validated Hg-methylating strain *Desulfovibrio desulfuricans* ND132 [5, 50]. Modelling of the Lokiarchaeota HgcB protein demonstrated two 4Fe-4S motifs at the N-terminal and the Cys tail at the C-terminal, with the function of transferring electrons and binding the Hg(II) substrate, respectively. Overall,
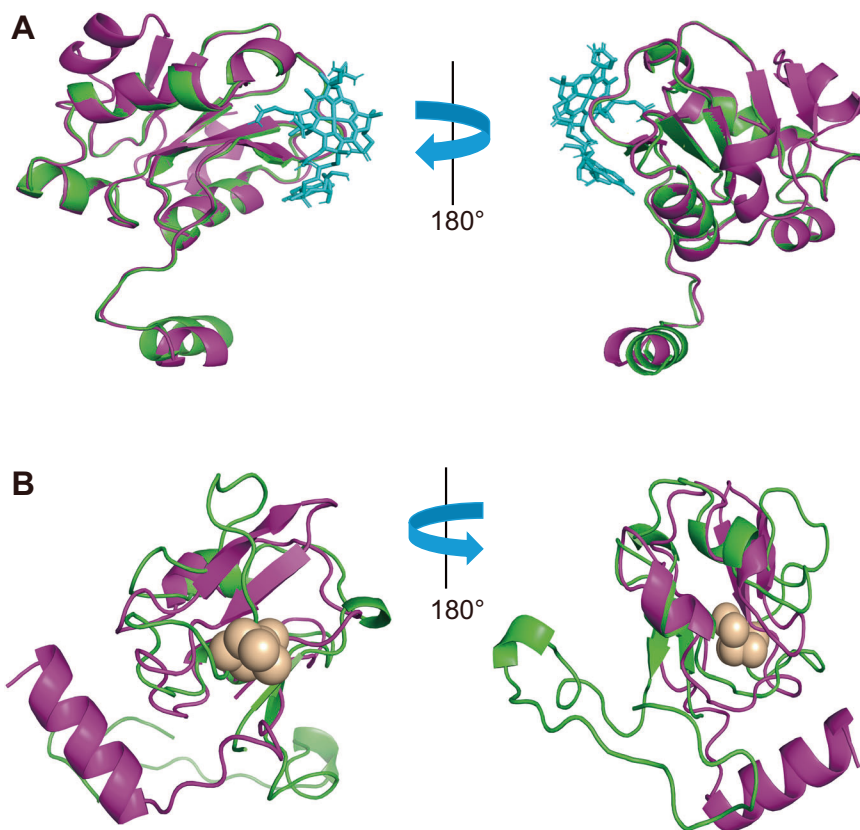
Fig. 3 Structure comparison between HgcA and HgcB from Lokiarchaeota and _Desulfovibrio desulfuricans_ ND132. A Superposition of Lokiarcheaota-HgcA (green) and _Desulfovibrio desulfuricans_ ND132-HgcA (purple) functional domain homology models. The functional domain is bound to cobalamin shown cyan-blue stick; **B** Superposition of Lokiarchaeota-HgcB (green) and _Desulfovibrio desulfuricans_ ND132-HgcB (purple) homology models. Model of full-length Lokiarchaeota-HgcB in complex with two [4Fe-4S] clusters; Interactions between the protein and iron are shown by brown ball.

our findings strongly suggest that Asgard archaea represent novel potential Hg-methylators. The extension of Hg methylators' phylogeny into Asgard also broadly expands the niches associated with MeHg production. Asgard archaea carrying _hgcA_ have been retrieved from a range of anoxic environments, including marine/coastal, lake environments, hydrothermal vent, cold seep, and permafrost sediments (Table S5), suggesting MeHg production by Asgard archaea across a wide range of ecological environments might be ignored previously.

Hg-methylation process includes reduction of the corrinoid cofactor to form Co(I), methylation of Co(I) to form CH_3-Co(III), and methyl transfer to Hg(II) to form $CH_3Hg(II)$. The presence of _hgcAB_ in Asgard archaea might be insufficient for Hg methylation, and additional genes functioning in uptake and transport of Hg(II) and MeHg export might be needed for effective MeHg production [50]. No experimental assays have been conducted for mercury methylation of Asgard archaea. Therefore, experimental confirmation of Hg-methylation capacity in Asgard archaea needs to be provided by future research.

Additional metabolic features of _hgcA_-carrying Asgard MAGs
The functional potentials of 104 _hgcA_-carrying Asgard MAGs were inferred by reference to eggNOGmapper annotations (Fig. S7, Table S7). Asgard lineages mostly inhabited anoxic marine, coastal, and lake sediments. However, some of them contained genes encoding for terminal oxidases, which allowed them to accommodate the lower levels of oxygen in the benthic habitats of shallow layers. Genome analysis reveals that Hod- and Kariarchaeota contain genes encoding for respiratory complexes cytochrome _c_ oxidase (_cox_BCP). Hodarchaeota also contain genes encoding for cytochrome

_bd_ ubiquinol oxidase (_cyd_AB). The presence of _cox_ and _cyd_ genes indicates that Hod- and Kariarchaeota might represent facultative aerobes under fluctuating oxygen conditions. Furthermore, genes encoding for flagellar proteins (_flg_, _fli_, and _mot_) were identified in Hermod-, Hod-, and Thorarchaeota, enabling them to reposition optimally to suitable O_2 levels.

Asgard archaea appear to have diverse metabolic capabilities in C, N, S cycles (Fig. S7, Table S7). The presence of an almost-complete archaeal Wood-Ljungdahl (WL) pathway and carbon monoxide dehydrogenase/acetyl-CoA synthase (CODH/ACS) in Borr-, Hela-, Hermoda-, Loki-, and Thorarchaeota suggests that they can fix CO_2 or, in a reverse function, produce it [51]. HgcA and the CODH have structural and functional similarities, suggesting associations between the two pathways [2]. Genes encoding for trimethylamine-specific methyltransferase (MttB) were found in Hermod-, Hod-, Loki-, and Thorarchaeota, suggesting they have potential for utilization of trimethylamine. Helarchaeota from marine and coastal sediments have acetyl-coenzyme M reductase (_acr_) coding genes, suggesting they have the potential for short-chain hydrocarbon oxidation [19, 23]. Kariarchaeota MAGs contain genes encoding nitrate reductase (Nar). Hel-, Hod-, and Thorarchaeota MAGs contain genes encoding nitrite reductase (Nir), suggesting nitrite can be a nitrogen source for them. We also detected the sulfate reduction–related genes _sat_ and _cys_ within most Asgard archaea. Above all, Hg methylators in Asgard are also involved in diverse metabolic functions and growth strategies.

Although MeHg is much more toxic than Hg(II), MeHg can be exported from the cell [52]. Similarly, As(V) is reduced to the more toxic As(III) to export from the cell. Hg methylation and As reduction are both detoxification mechanisms deployed against environmental
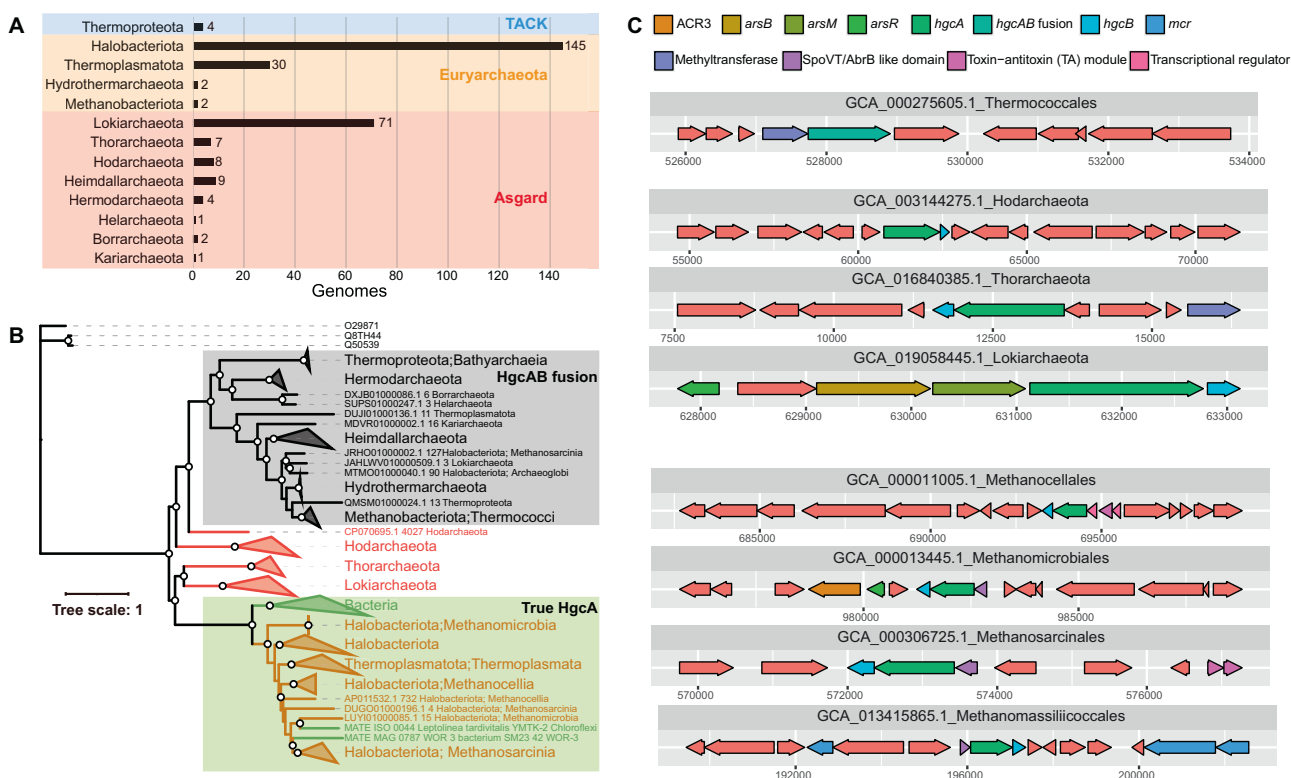
Fig. 4   Diversity and phylogenetic analyses of archaeal HgcA amino acid sequences. A Numbers of putative methylating genomes belonging to each taxa. **B** Maximum-likelihood phylogenetic tree of HgcA amino acid sequences (1000 bootstraps; values >90% are shown by white dots at the nodes). Gray-shaded clades represent the fused HgcAB sequences. Green-shaded clades represent the true HgcA sequences. HgcA sequences belonging to Euryarchaeota and Asgard are represented by orange and red, respectively. **C** Gene clusters of contigs containing *hgcA* in various archaeal taxa. Colors correspond to predicted functions of each gene. HgcAB sequences were identified based on HMMs, while all other genes were based on prodigal predictions.

stress. In our study, most methylators in Asgard also contained genes encoding for arsenate reductase (Ars), Cu transport detoxification protein (CopA), and Fe^{2+} transport system protein (FeoAB) (Table S7), protecting them against other toxin compounds. Interestingly, we selected several Lokiarchaeota MAGs containing *hgcAB* and *ars* regions and found *ars* were in the neighborhood of *hgcAB* within the same scaffolds (Fig. S8, Table S8). Gene clusters *hgcAB* were flanked by *arsR*, encoding an arsenical resistance operon repressor; *arsB*, encoding an arsenical pump membrane protein; *arsM*, an arsenite S-adenosylmethionine methyltransferase; *arsC*, encoding a thioredoxin- or glutaredoxin-dependent arsenite reductase; and *arsA*, encoding arsenite-activated ATPase. The potential for metal resistance and transformation may allow Asgard to adapt to metal-containing environments.

The diversity of archaeal *hgcA* carriers
To investigate the diversity of *hgcAB* genes in archaea, we searched publicly available archaeal isolate genomes and MAGs and obtained 287 archaeal potential Hg methylators (Table S9). The 287 archaeal *hgcA*-carriers belongs to three superphyla: TACK, Euryarchaeota, and Asgard (Fig. 4A). HgcA-encoding genes were found less frequently in TACK. HgcA-encoding genes were found in Bathyarchaeia and Thermoproteia in TACK. The occurrence of *hgcAB* among Euryarchaeota was confined to seven classes: Archaeoglobi, Methanocellia, Methanomicrobia, Methanosarcinia, Hydrothermarchaeia, Thermococci, and Thermoplasmata. Methanocellia with *hgcAB* are widespread in rice paddies [53], and *Methanomassiliicoccus luminyensis* with *hgcAB* was isolated from human feces [54], suggesting a potential human health risk. Some *hgcA*-carriers in Methanomicrobia, Methanosarcinia, and Methanomassiliicoccales were obtained from permafrost soils,

which also need further attention concerning elevated Hg deposition in the Arctic ecosystem [55]. This study remarkably expands the diversity and distribution of known *hgcA*-carriers in the domain Archaea.

A phylogenetic tree was constructed of HgcA amino acid sequences from 287 archaeal *hgcA*-carrying MAGs and 3 HgcA paralogues from non-methylating microorganisms (Fig. 4B). According to the phylogeny, some *hgcA* and *hgcB* sequences are fused into a single open reading frame in 30 *hgcA*-carrying genomes (Table S9), as shown in the gray-shaded clades in Fig. 4B. Among these, only two (*Methanococcoides methylutens* and *Pyrococcus furiosus*) were cultured organisms, which were experimentally validated to be unable to produce MeHg, indicating that the fused HgcAB may not retain the function of Hg methylation [2, 56]. HgcA from five Asgard phyla (Borrarchaeota, Kariarchaeota, Heimdallarchaeota, Helarchaeota, and Hermodarchaeota) were fused with HgcB sequences. Most *hgcA* fusion carriers were obtained from extreme environments, including a hydrothermal vent and a saline lake (Table S9). Some HgcA amino acid sequences from three Asgard phyla (Hod-, Loki-, and Thorarchaeota) were in a transitional stage between fused HgcAB and true HgcA, which have implications for the underlying evolutionary mechanisms of the methylation pathway (Fig. 4B). Experimental confirmation of Hg-methylation capacity in Asgard archaea could be launched to fill this gap. Since HgcA and carbon monoxide dehydrogenase/acetyl-CoA synthase gamma subunit (CFeSP) had the paralogous relationship, we constructed phylogenetic tree of CFeSP (Fig. S9). We found CFeSP in Euryarchaeota appear in all clades, suggesting CFeSP might originate from Euryarchaeota, which is consistent with previous propose [2]. Microorganisms with syntrophic interactions acquired *hgcAB* through HGT.

We provided the blast hits of 291 HgcA amino acid sequences to the 32 experimentally confirmed HgcA sequences (Table S10). Corresponded to the phylogenetic tree, HgcAB fusion clade sequences had a lower identity (<47%) and lower align length (<266 bp). Asgard HgcA clade sequences had a lower identity (<47%) and higher align length (>268 bp). Euryarchaeota and bacterial true HgcA clade sequences had a higher identity (>50%) and higher align length (>266 bp). Moreover, contig synteny (Fig. 4C) was combined with a phylogenetic tree (Fig. 4B). The contig synteny varied among the three clades (Table S11). HgcAB fusion-containing contigs contained methyltransferase. Asgard HgcA-containing contigs contained methyltransferase and Ars-related proteins. Euryarchaeota true HgcA-containing contigs contained Ars-related proteins, SpoVT/AbrB like domain and toxin-antitoxin (TA) module. The variation of gene clusters have an implication for evolution of Hg methylation function.

In summary, MeHg concentrations and *hgcA* gene abundances were reported, and both were highest in Shenzhen mangrove sediments. A total of 157 *hgcA*-carrying MAGs from mangrove sediments and 104 additional Asgard *hgcA*-carrying MAGs from publicly available databases were obtained. According to the relative abundance and expression of these Hg-methylators, Deltaproteobacteria, Euryarchaeota, Bacteroidetes, Chloroflexi were the most abundant and transcriptionally active Hg-methylating groups, suggesting that they could contribute most to the MeHg production in mangrove sediments. Multiple lines of evidence support the conclusion that Asgard are previously unrecognized microbial Hg-methylators. Further studies should experimentally confirm Hg-methylation function in Lokiarchaeota enrichments.

MATERIALS AND METHODS
Sampling and chemical analysis
A total of 83 sediment samples were collected from six mangrove nature reserves: Ximendao National Marine Reserve in Zhejiang Province (XMD), Yunxiao Zhangjiangkou National Nature Reserve in Fujian Province (YX), Shenzhen Futian National Nature Reserve in Guangdong Province (SZ), Leizhou Nature Reserve in Guangdong Province (LZ), Dongzhaigang National Nature Reserve in Hainan Province (DZG), and Danzhou Xinyinggang Nature Reserve in Hainan Province (DZ) (Fig. S1, Table S1). Sediment samples in XMD, YX, LZ, DZG, and DZ were collected from October to December 2017 and stored at −40 °C. In SZ, samples from 0–2, 6–8, 12–14, 20–22, and 28–30 cm of a 32 cm sediment core were collected in April 2017 and stored at −40 °C. The physiochemical properties of these sediments were distinct from one another, as reported previously [57, 58]. Total Hg (THg) and methylmercury (MeHg) contents in the sediments were measured as previously [29]. Among all the samples, 10 representative sediment samples (bold in Table S1) were chosen for metagenomics sequencing. Three subsurface samples in XMD, YX, LZ, DZG, and DZ were combined as one sample, respectively.

Nucleic acid extraction, metagenome/metatranscriptome sequencing and assembly
Genomic DNA was extracted from 5 g of wet sediment samples using DNeasy PowerSoil kit (Qiagen, Germany) according to the manufacturer's protocol. Shotgun metagenomic sequencing (2 × 150 bp) of the above 10 samples was performed using HiSeq 2000 (Illumina, USA) at Novogene Bioinformatics Technology Co., Ltd. (Tianjin, China). About 110 Gbp of sequence data were generated for each sample. For each sample, raw reads of metagenomic datasets (2 × 150 bp paired-end) were dereplicated and trimmed to remove replicated and low-quality reads using Sickle (https://github.com/najoshi/sickle) with the default settings. The trimmed reads were de novo assembled into longer scaffolds using IDBA-UD (v1.1.1) with the following parameters: -mink 65, -maxk 145, and -step 10 [59]. For five sediment samples in SZ, the trimmed reads were co-assembled using MEGAHIT v1.2.8 [60]. The assembled scaffolds longer than 500 bp were translated by Prodigal (v.2.6.3) using the "-p meta" parameters [61]. RNA extraction and metatranscriptomic analysis from the 0–2, 6–8, and 12–14 cm layers in SZ has been described in a previous study [62].

Metagenomic binning and annotation
Assembled scaffolds were binned using MetaBAT (v.2.12.1) [63], then aggregated using DAS Tool [64]. The completeness, contamination, and strain heterogeneity of recovered MAGs were evaluated by using CheckM (v1.0.11) [65]. Only those bins which were of medium to high quality (i.e., ≥50% complete, <10% contaminated) were analyzed further. The MAGs obtained from six sites were dereplicated using dRep (v2.5.4) [66] at 97% cutoff. After dereplication, we retrieved 125 bins in XMD, 96 bins in YX, 89 bins in LZ, 100 bins in DZG, 68 bins in DZ, and 705 bins in SZ. The dereplicated bins were selected for further analysis. The taxonomy of each bin was estimated using GTDB-Tk (v1.5.0) [67]. The MAGs were translated by Prodigal using the "-p meta" parameters and annotated using the KEGG Automatic Annotation Server (www.genome.jp/tools/kaas/) [68] and eggNOG-mapper (http://eggnog-mapper.embl.de/) [69].

Identification of *hgcAB*
The *hgcAB* gene identification in shotgun metagenomics datasets using HMM is a reliable method for determining Hg-methylator abundance and diversity [13]. A custom HMM of the HgcA sequence was built with hmmbuild from the hmmer softerware [70] using HgcA amino acid sequences with and without experimental validation from Hg-MATE database [39] as reference. Putative *hgcA* sequences were searched from each assembly using hmmsearch (v3.1b2) [71] with score >131.8 and *E* value ≤ 1e−05 as the cutoff. Each hit was then manually confirmed by validating the presence of conserved sequence domains (cap helix domain (N(V/I)WCA(A/G) and at least four transmembrane domains) [5]. The transmembrane domains were predicted by TMHMM (http://www.cbs.dtu.dk/services/TMHMM/). Sequences annotated as *hgcA* were extracted, resulting in 1087 *hgcA* sequences (Table S2). The genes immediately downstream of each *hgcA* gene were extracted, and sequences that contained the conserved CX2CX2CX3C motif were scored as *hgcB* genes. HgcA sequences that binned to MAGs were assigned taxonomic classifications according to GTDB taxonomy of MAGs phylogenies. Those HgcA sequences that not binned to MAGs were searched against reference HgcA and HgcAB sequences database published recently [39] using BLASTp (Table S3).

Phylogenetic analysis
For HgcA phylogenies, putative HgcA amino acid sequences and reference HgcA sequences [39] were aligned using MUSCLE (v3.8.31) [72] and trimmed using trimAL with option "-gt 0.95" [73]. The HgcA maximum likelihood (ML) tree was constructed with IQ-TREE (v1.3.10) [74] under the LG + F + G4 protein model chosen according to BIC [75] with option "-bb 1000".

We also investigated the phylogenetic relationship between HgcA and the gamma subunit of the acetyl-CoA synthase complex (CFeSP) involved in the WL pathway. The MAGs were translated by Prodigal using the "-p meta" parameters and annotated using the KEGG Automatic Annotation Server (www.genome.jp/tools/kaas/). CFeSP corresponds to KO number K00197. The CFeSP ML tree was conducted with IQ-TREE (v1.3.10) under the LG + F + G4 protein model chosen according to BIC with option "-bb 1000". All trees were visualized by using iTOL [76].

Protein homology modeling
The amino acid sequences of HgcA and HgcB was extracted from the 'Candidatus Prometheoarchaeum syntrophicum' strain MK-D1 and Desulfovibrio desulfuricans ND132 genomes. Computational homology modeling was performed to identify novel Asgard Hg-methylators. The three-dimensional structures of the putative HgcA and HgcB sequences were built using AlphaFold [77]. The cobalamin and [4Fe-4S] clusters were docked to the HgcA and HgcB using AutoDock VinA [78], respectively. All of the structure were visualized, and exported as images using PyMOL (http://www.pymol.org).

Relative abundance and expression of *hgcA*-carrying MAGs and *hgcA* genes
The 157 *hgcA*-carrying MAGs and 1087 *hgcA* gene sequences were used to recruit reads from metagenomics and metatranscriptomic datasets to calculate relative abundance and expression, respectively. The abundance/expression of dereplicated MAGs was estimated by mapping the metagenomic/metatranscriptomic reads, respectively, to the contigs of the MAGs using Bowtie2 (v2.2.8) [79]. BEDTools was applied to calculate coverage values for the contigs [80]. The relative abundance of each *hgcA*-carrying MAG is defined as the number of reads mapped to individual *hgcA*-carrying MAG divided by the total number of metagenomic/metatranscriptomic reads mapped to all *hgcA*-carrying MAGs in every sample.

The abundance and transcription of *hgcA* genes were determined by mapping metagenomic/metatranscriptomic reads to annotated *hgcA* gene sequences using Burrows-Wheeler Aligner (BWA, v0.7.5a-r405) with default settings [81]. The read coverage in genes was calculated using BEDTools. The mapped reads were then normalized to the length of the gene and the number of mapped reads using the "Fragments per kilobase per million" or "FPKM" metric. For *hgcA*, the relative abundance of each group was calculated by dividing the FPKM value of the individual group by the sum of FPKM values of all groups.

Explore the diversity of archaeal *hgcA* carriers

To investigate the diversity of *hgcAB* genes in archaea, we downloaded publicly available archaeal metagenome-assembled genomes (MAGs) from the GenBank database in December 2021. Using the criteria described above, we identified 287 *hgcA*-carrying archaeal MAGs, including 104 *hgcA*-carrying Asgard, 4 TACK, and 179 Euryarchaeota genomes, from this data set. The taxonomy of archaeal MAGs was estimated using GTDB-Tk (v1.5.0) [67].

DATA AVAILABILITY

The genome bins generated and analyzed during the current study are available in the National Omics Data Encyclopedia (NODE, https://www.biosino.org/node/) database and can be viewed under Project OEP003752. The HgcAB amino acid sequences, and their alignment and phylogenetic tree have also been uploaded to the NODE database under Project OEP003752. The metagenome and metatranscriptome raw data generated during the current study can be viewed in NODE under Project OEP001892 and OEP000712.

CODE AVAILABILITY

The sources of the code and programs used for analyses are mentioned in the Methods, and are also available at GitHub (https://github.com/cui-jing/Mangrove-hgcAB).

REFERENCES

1. Hsu-Kim H, Kucharzyk KH, Zhang T, Deshusses MA. Mechanisms regulating mercury bioavailability for methylating microorganisms in the aquatic environment: A critical review. Environ Sci Technol. 2013;47:2441–56.
2. Podar M, Gilmour CC, Brandt CC, Soren A, Brown SD, Crable BR, et al. Global prevalence and distribution of genes and microorganisms involved in mercury methylation. Sci Adv. 2015;1:e1500675.
3. Liu YR, Johs A, Bi L, Lu X, Hu HW, Sun D, et al. Unraveling microbial communities associated with methylmercury production in paddy soils. Environ Sci Technol. 2018;52:13110–8.
4. Lee C-S, Fisher NS. Bioaccumulation of methylmercury in a marine copepod. Environ Toxicol Chem. 2017;36:1287–93.
5. Parks JM, Johs A, Podar M, Bridou R, Hurt RAJ, Smith SD, et al. The genetic basis for bacterial mercury methylation. Science 2013;339:1332–5.
6. McDaniel EA, Peterson BD, Stevens SLR, Tran PQ, Anantharaman K, McMahon KD. Expanded phylogenetic diversity and metabolic flexibility of mercury-methylating microorganisms. mSystems 2020;5:e00299–20.
7. Cooper CJ, Zheng K, Rush KW, Johs A, Sanders BC, Pavlopoulos GA, et al. Structure determination of the HgcAB complex using metagenome sequence data: Insights into microbial mercury methylation. Commun Biol. 2020;3:320.
8. Kerin EJ, Gilmour CC, Roden E, Suzuki MT, Coates JD, Mason RP. Mercury methylation by dissimilatory iron-reducing bacteria. Appl Environ Microbiol. 2006;72:7919–21.
9. Gilmour CC, Podar M, Bullock AL, Graham AM, Brown SD, Somenahally AC, et al. Mercury methylation by novel microorganisms from new environments. Environ Sci Technol. 2013;47:11810–20.
10. Capo E, Bravo AG, Soerensen AL, Bertilsson S, Pinhassi J, Feng C, et al. Delta-proteobacteria and Spirochaetes-like bacteria are abundant putative mercury methylators in oxygen-deficient water and marine particles in the Baltic Sea. Front Microbiol. 2020;11:574080.
11. Gionfriddo CM, Tate MT, Wick RR, Schultz MB, Zemla A, Thelen MP, et al. Microbial mercury methylation in Antarctic sea ice. Nat Microbiol. 2016;1:16127.
12. Jones DS, Walker GM, Johnson NW, Mitchell CPJ, Coleman Wasik JK, Bailey JV. Molecular evidence for novel mercury methylating microorganisms in sulfate-impacted lakes. ISME J. 2019;13:1659–75.
13. Christensen GA, Gionfriddo CM, King AJ, Moberly JG, Miller CL, Somenahally AC, et al. Determining the reliability of measuring mercury cycling gene abundance with correlations with mercury and methylmercury concentrations. Environ Sci Technol. 2019;53:8649–63.
14. Villar E, Cabrol L, Heimburger-Boavida LE. Widespread microbial mercury methylation genes in the global ocean. Environ Microbiol Rep. 2020;12:277–87.
15. Lin H, Ascher DB, Myung Y, Lamborg CH, Hallam SJ, Gionfriddo CM, et al. Mercury methylation by metabolically versatile and cosmopolitan marine bacteria. ISME J. 2021;15:1810–25.
16. King JK, Kostka JE, Frischer ME, Saunders FM, Jahnke RA. A quantitative relationship that demonstrates mercury methylation rates in marine sediments are based on the community composition and activity of sulfate-reducing bacteria. Environ Sci Technol. 2001;35:2491–6.
17. Regnell O, Watras CJ. Microbial mercury methylation in aquatic environments: A critical review of published field and laboratory studies. Environ Sci Technol. 2019;53:4–19.
18. Xie R, Wang Y, Huang D, Hou J, Li L, Hu H, et al. Expanding Asgard members in the domain of Archaea sheds new light on the origin of eukaryotes. Sci China Life Sci. 2022;65:818–29.
19. Seitz KW, Dombrowski N, Eme L, Spang A, Lombard J, Sieber JR, et al. Asgard archaea capable of anaerobic hydrocarbon cycling. Nat Commun. 2019;10:1822.
20. Zaremba-Niedzwiedzka K, Caceres EF, Saw JH, Backstrom D, Juzokaite L, Vancaester E, et al. Asgard archaea illuminate the origin of eukaryotic cellular complexity. Nature 2017;541:353–8.
21. Liu Y, Makarova KS, Huang W-C, Wolf YI, Nikolskaya AN, Zhang X, et al. Expanded diversity of Asgard archaea and their relationships with eukaryotes. Nature 2021;593:553–7.
22. Zhang JW, Dong HP, Hou LJ, Liu Y, Ou YF, Zheng YL, et al. Newly discovered Asgard archaea Hermodarchaeota potentially degrade alkanes and aromatics via alkyl/benzyl-succinate synthase and benzoyl-CoA pathway. ISME J. 2021;15:1826–43.
23. Cai M, Liu Y, Yin X, Zhou Z, Friedrich MW, Richter-Heitmann T, et al. Diverse Asgard archaea including the novel phylum Gerdarchaeota participate in organic matter degradation. Sci China Life Sci. 2020;63:886–97.
24. Baker BJ, De Anda V, Seitz KW, Dombrowski N, Santoro AE, Lloyd KG. Diversity, ecology and evolution of Archaea. Nat Microbiol. 2020;5:887–900.
25. Farag Ibrahim F, Zhao R, Biddle Jennifer F, Atomi H. "Sifarchaeota," a novel Asgard phylum from Costa Rican sediment capable of polysaccharide degradation and anaerobic methylotrophy. Appl Environ Micro. 2021;87:e02584–20.
26. Adam PS, Borrel G, Brochier-Armanet C, Gribaldo S. The growing tree of Archaea: new perspectives on their diversity, evolution and ecology. ISME J. 2017;11:2407–25.
27. Cai M, Richter-Heitmann T, Yin X, Huang W-C, Yang Y, Zhang C, et al. Ecological features and global distribution of Asgard archaea. Sci Total Environ. 2021; 758:143581.
28. Zhang C-J, Chen Y-L, Sun Y-H, Pan J, Cai M-W, Li M. Diversity, metabolism and cultivation of archaea in mangrove ecosystems. Mar Life Sci Tech. 2020;3:252–62.
29. Dai SS, Yang Z, Tong Y, Chen L, Liu SY, Pan R, et al. Global distribution and environmental drivers of methylmercury production in sediments. J Hazard Mater. 2021;407:124700.
30. Tang WL, Liu YR, Guan WY, Zhong H, Qu XM, Zhang T. Understanding mercury methylation in the changing environment: Recent advances in assessing microbial methylators and mercury bioavailability. Sci Total Environ. 2020;714:136827.
31. Tsui MTK, Finlay JC, Balogh SJ, Nollet YH. In situ production of methylmercury within a stream channel in northern California. Environ Sci Technol. 2010;44:6998–7004.
32. Liu Y, Zhou Z, Pan J, Baker BJ, Gu JD, Li M. Comparative genomic inference suggests mixotrophic lifestyle for Thorarchaeota. ISME J. 2018;12:1021–31.
33. Lei P, Zhong H, Duan D, Pan K. A review on mercury biogeochemistry in mangrove sediments: Hotspots of methylmercury production? Sci Total Environ. 2019;680:140–50.
34. Beckers F, Rinklebe J. Cycling of mercury in the environment: Sources, fate, and human health implications: A review. Crit Rev Env Sci Tec. 2017;47:693–794.
35. de Oliveira DC, Correia RR, Marinho CC, Guimaraes JR. Mercury methylation in sediments of a Brazilian mangrove under different vegetation covers and salinities. Chemosphere 2015;127:214–21.
36. Li R, Xu H, Chai M, Qiu GY. Distribution and accumulation of mercury and copper in mangrove sediments in Shenzhen, the world's most rapid urbanized city. Environ Moni Assess. 2016;188:87.
37. O'Connor D, Hou D, Ok YS, Mulder J, Duan L, Wu Q, et al. Mercury speciation, transformation, and transportation in soils, atmospheric flux, and implications for risk management: A critical review. Environ Int. 2019;126:747–61.
38. Obrist D, Kirk JL, Zhang L, Sunderland EM, Jiskra M, Selin NE. A review of global environmental mercury processes in response to human and natural perturbations: Changes of emissions, climate, and land use. Ambio 2018;47:116–40.
39. Capo E, Peterson BD, Kim M, Jones DS, Acinas SG, Amyot M, et al. A consensus protocol for the recovery of mercury methylation genes from metagenomes. Mol Ecol Resour. 2022; https://doi.org/10.1111/1755-0998.13687.
40. Gionfriddo CM, Wymore AM, Jones DS, Wilpiszeski RL, Lynes MM, Christensen GA, et al. An improved *hgcAB* primer set and direct high-throughput sequencing expand Hg-methylator diversity in nature. Front Microbiol. 2020;11:541554.
41. Yu R-Q, Barkay T. Chapter two - microbial mercury transformations: Molecules, functions and organisms. Adv Appl Microbiol. 2022;118:31–90.

42. Chételat J, Richardson MC, MacMillan GA, Amyot M, Poulain AJ. Ratio of methylmercury to dissolved organic carbon in water explains methylmercury bioaccumulation across a latitudinal gradient from north-temperate to arctic lakes. Environ Sci Technol. 2018;52:79–88.

43. Liu Y-R, Dong J-X, Han L-L, Zheng Y-M, He J-Z. Influence of rice straw amendment on mercury methylation and nitrification in paddy soils. Environ Pollut. 2016;209:53–9.

44. Moreau JW, Gionfriddo CM, Krabbenhoft DP, Ogorek JM, DeWild JF, Aiken GR, et al. The effect of natural organic matter on mercury methylation by *Desulfobulbus propionicus* 1pr3. Front Microbiol. 2015;6:1389.

45. Chen C-F, Ju Y-R, Chen C-W, Dong C-D. The distribution of methylmercury in estuary and harbor sediments. Sci Total Environ. 2019;691:55–63.

46. Bravo AG, Bouchet S, Guédron S, Amouroux D, Dominik J, Zopfi J. High methylmercury production under ferruginous conditions in sediments impacted by sewage treatment plant discharges. Water Res. 2015;80:245–55.

47. Wang H, Su J, Zheng T, Yang X. Insights into the role of plant on ammonia-oxidizing bacteria and archaea in the mangrove ecosystem. J Soil Sediment. 2015;15:1212–23.

48. Imachi H, Nobu MK, Nakahara N, Morono Y, Ogawara M, Takaki Y, et al. Isolation of an archaeon at the prokaryote–eukaryote interface. Nature 2020;577:519–25.

49. Zhou J, Riccardi D, Beste A, Smith JC, Parks JM. Mercury methylation by HgcA: Theory supports carbanion transfer to Hg(II). Inorg Chem. 2014;53:772–7.

50. Smith Steven D, Bridou R, Johs A, Parks Jerry M, Elias Dwayne A, Hurt Richard A, et al. Site-directed mutagenesis of HgcA and HgcB reveals amino acid residues important for mercury methylation. Appl Environ Micro. 2015;81:3205–17.

51. Sousa FL, Neukirchen S, Allen JF, Lane N, Martin WF. Lokiarchaeon is hydrogen dependent. Nat Microbiol. 2016;1:16034.

52. Schaefer JK, Rocks SS, Zheng W, Liang L, Gu B, Morel FMM. Active transport, substrate specificity, and methylation of Hg(II) in anaerobic bacteria. Proc Natl Acad Sci USA 2011;108:8714.

53. Sakai S, Imachi H, Hanada S, Ohashi A, Harada H, Kamagata Y. *Methanocella paludicola* gen. nov., sp. nov., a methane-producing archaeon, the first isolate of the lineage 'Rice Cluster I', and proposal of the new archaeal order *Methanocellales* ord. nov. Int J Syst Evol Microbiol. 2008;58:929–36.

54. Dridi B, Fardeau ML, Ollivier B, Raoult D, Drancourt M. *Methanomassiliicoccus luminyensis* gen. nov., sp. nov., a methanogenic archaeon isolated from human faeces. Int J Syst Evol Microbiol. 2012;62:1902–7.

55. Dietz R, Sonne C, Basu N, Braune B, O'Hara T, Letcher RJ, et al. What are the toxicological effects of mercury in arctic biota? Sci Total Environ. 2013;443:775–90.

56. Gilmour Cynthia C, Bullock Allyson L, McBurney A, Podar M, Elias Dwayne A, Lovley Derek R. Robust mercury methylation across diverse methanogenic archaea. mBio 2018;9:e02403–17.

57. Pan J, Chen Y, Wang Y, Zhou Z, Li M. Vertical distribution of Bathyarchaeotal communities in mangrove wetlands suggests distinct niche preference of Bathyarchaeota subgroup 6. Micro Ecol. 2019;77:417–28.

58. Zhang C-J, Pan J, Duan C-H, Wang Y-M, Liu Y, Sun J, et al. Prokaryotic diversity in mangrove sediments across southeastern China fundamentally differs from that in other biomes. mSystems 2019;4:e00442–19.

59. Peng Y, Leung HC, Yiu SM, Chin FY. IDBA-UD: a *de novo* assembler for single-cell and metagenomic sequencing data with highly uneven depth. Bioinformatics 2012;28:1420–8.

60. Li D, Liu C-M, Luo R, Sadakane K, Lam T-W. MEGAHIT: an ultra-fast single-node solution for large and complex metagenomics assembly via succinct de Bruijn graph. Bioinformatics 2015;31:1674–6.

61. Hyatt D, Chen G-L, LoCascio PF, Land ML, Larimer FW, Hauser LJ. Prodigal: prokaryotic gene recognition and translation initiation site identification. BMC Bioinforma. 2010;11:119.

62. Zhang C-J, Pan J, Liu Y, Duan C-H, Li M. Genomic and transcriptomic insights into methanogenesis potential of novel methanogens from mangrove sediments. Microbiome. 2020;8:94.

63. Kang DD, Froula J, Egan R, Wang Z. MetaBAT, an efficient tool for accurately reconstructing single genomes from complex microbial communities. PeerJ 2015;3:e1165.

64. Sieber CMK, Probst AJ, Sharrar A, Thomas BC, Hess M, Tringe SG, et al. Recovery of genomes from metagenomes via a dereplication, aggregation and scoring strategy. Nat Microbiol. 2018;3:836–43.

65. Parks DH, Imelfort M, Skennerton CT, Hugenholtz P, Tyson GW. CheckM: assessing the quality of microbial genomes recovered from isolates, single cells, and metagenomes. Genome Res. 2015;25:1043–55.

66. Olm MR, Brown CT, Brooks B, Banfield JF. dRep: A tool for fast and accurate genomic comparisons that enables improved genome recovery from metagenomes through de-replication. ISME J. 2017;11:2864–8.

67. Chaumeil PA, Mussig AJ, Hugenholtz P, Parks DH. GTDB-Tk: a toolkit to classify genomes with the Genome Taxonomy Database. Bioinformatics 2019;36:1925–7.

68. Kanehisa M, Sato Y, Morishima K. BlastKOALA and GhostKOALA: KEGG tools for functional characterization of genome and metagenome sequences. J Mol Biol. 2016;428:726–31.

69. Huerta-Cepas J, Forslund K, Szklarczyk D, Jensen LJ, von Mering C, Bork P. Fast genome-wide functional annotation through orthology assignment by eggNOG-mapper. Mol Biol Evol. 2017;34:2115–22.

70. Finn RD, Clements J, Eddy SR. HMMER web server: interactive sequence similarity searching. Nucleic Acids Res. 2011;39:W29–W37.

71. Eddy SR. Accelerated profile HMM searches. PLoS Comput Biol. 2011;7:e1002195.

72. Edgar RC. MUSCLE: Multiple sequence alignment with high accuracy and high throughput. Nucleic Acids Res. 2004;32:1792–7.

73. Capella-Gutiérrez S, Silla-Martínez JM, Gabaldón T. trimAl: a tool for automated alignment trimming in large-scale phylogenetic analyses. Bioinformatics 2009;25:1972–3.

74. Nguyen L-T, Schmidt HA, von Haeseler A, Minh BQ. IQ-TREE: a fast and effective stochastic algorithm for estimating maximum-likelihood phylogenies. Mol Biol Evol. 2015;32:268–74.

75. Price MN, Dehal PS, Arkin AP. FastTree 2 – approximately maximum-likelihood trees for large alignments. Plos ONE. 2010;5:e9490.

76. Letunic I, Bork P. Interactive tree of life (iTOL) v3: an online tool for the display and annotation of phylogenetic and other trees. Nucleic Acids Res. 2016;44:W242–5.

77. Jumper J, Evans R, Pritzel A, Green T, Figurnov M, Ronneberger O, et al. Highly accurate protein structure prediction with AlphaFold. Nature 2021;596:583–9.

78. Trott O, Olson AJ. AutoDock Vina: Improving the speed and accuracy of docking with a new scoring function, efficient optimization, and multithreading. J Comput Chem. 2010;31:455–61.

79. Langmead B, Salzberg SL. Fast gapped-read alignment with Bowtie 2. Nat Methods. 2012;9:357–9.

80. Quinlan AR, Hall IM. BEDTools: a flexible suite of utilities for comparing genomic features. Bioinforma (Oxf, Engl). 2010;26:841–2.

81. Li H, Durbin R. Fast and accurate short read alignment with Burrows-Wheeler transform. Bioinformatics 2009;25:1754–60.

ACKNOWLEDGEMENTS

AUTHOR CONTRIBUTIONS

C-JZ, Y-RL and ML conceived this study. C-JZ, YL, JP and MC performed sampling, DNA extraction and the data analyses. GC and ZL performed protein structure computation. X-QZ performed the laboratory measurement of physiochemical properties and Hg concentrations. C-JZ wrote, and all authors edited and approved the paper.

COMPETING INTERESTS

The authors declare no competing interests.

ADDITIONAL INFORMATION

Supplementary information The online version contains supplementary material available at https://doi.org/10.1038/s41396-023-01360-w.

Correspondence and requests for materials should be addressed to Meng Li.

Reprints and permission information is available at http://www.nature.com/reprints